Considerations on wireless light communications based on the Wi-Fi IEEE 802.11bb Amendment

Mike Wolf and Martin Haardt
Communications Research Laboratory,
Technische Universität Ilmenau, 98693 Ilmenau, Germany,
Email: mike.wolf@tu-ilmenau.de

***Abstract*—The 802.11bb$^{\mathrm{TM}}$ standard extended the Wi-Fi family to include the possibility of using the near-infrared spectrum. While this might seem like a simple matter of replacing a few analog components like antennas and amplifiers with optical counterparts, in reality it is more complex, as intensity modulation and direct detection replace coherent transmission, i.e., homodyne up- and down-conversion. In this article, we establish the relation between the required optical power and the electrical signal-to-noise ratio (SNR) which is otherwise often considered in isolation. We demonstrate that RF and "Light Communication" receivers also differ significantly with respect to noise sources and provide comparative examples of receiver sensitivity for common combinations of modulation and coding according to the 802.11n, 802.11ac, and 802.11ax standards.**

***Index Terms*—IEEE 802.11bb, Wi-Fi, Li-Fi, wireless optical communications, wireless infrared communications**

I. Introduction

In 2023, the IEEE Standards Association added the Amendment 6: Light Communications (IEEE 802.11bb-2023$^{\mathrm{TM}}$) to the IEEE 802.11 standards family [1]. This adds the possibility for Wi-Fi devices to use an optical frequency band in addition to the radio frequency (RF) bands. For "light communication" (LC), the standard specifies the wavelength range between 800 nm and 1000 nm. However, for LC, there is no equivalent to the homodyne up- and down-conversion that is used in RF. Instead, the optical signal (the emitted radiation) will be generated by varying the instantaneous power of a LED or laser diode, i.e., by intensity modulation (IM). At the receiver, direct detection (DD), is used, in which a photodetector (PIN photodiode or APD) generates a current that is proportional to the received instantaneous optical power. The information to be transmitted is thus contained in the instantaneous optical power. In fact, due to the limited coherence of the optical transmitters, the signals themselves are modeled as instantaneous optical powers $p(t)$. The required average power P at the receiver, as an important parameter that determines the link budget, is thus the linear average of the received signal $p(t)$ and not the mean squared value.

The idea behind the LC PHY is certainly to use the highly advanced baseband digital signal processing for modulation, coding, synchronization, and channel estimation of the RF PHY and to replace — more or less — only the analog RF components such as mixers, amplifiers and antennas.

For intensity modulation, the complex OFDM baseband signal must first be converted into a real-valued *electrical* passband signal via quadrature up-conversion. Since this yields a zero mean signal, a sufficiently large DC bias must be added in a second step prior to the LED (or laser) direct modulation. The instantaneous optical power which needs to fulfill the non-negative constraint $p(t) \geq 0$ is then, in the best case, proportional to the forward current which oscillates around the DC bias. The center frequency, which is used for the up-conversion on the electrical subcarrier, could theoretically be only slightly larger than half of the bandwidth of the complex baseband signal. However, to operate a network with multiple access points (APs), several frequency bands are available and defined in the range between a minimum of 16 MHz and a maximum of 336 MHz [1]. For 20, 40, and 80 MHz waveforms, for example, the lowest possible subcarrier center frequencies f_{c} are 26, 36 and 56 MHz.

In this article, we aim to evaluate the LC-PHY, but we do not take multipath propagation into account. The goal is to identify practical issues that may (and will) arise during implementation and to evaluate the receiver sensitivity. For the RF High-Throughput (HT), Very-High-Throughput (VHT), and High-Efficiency (HE) PHYs, the receiver sensitivities, which must be met as a minimum, are precisely specified in the relevant standards 802.11n (Wi-Fi4), 802.11ac (Wi-Fi5), and 802.11ax (Wi-Fi6) depending on the bandwidth and the modulation and coding scheme (MCS) [2], [3]. The LC Amendment, however, only specifies a "general" minimum receiver sensitivity of -15 dBm that must be met.

In the following Section II, we present our assumptions regarding the transmitter (Tx) and receiver (Rx), where we focus on the components that are specific to the LC PHY. In Section III, we analyze the *optical* power efficiency of the various Wi-Fi MCSs in the context of IM/DD. We will also derive an estimation of the required optical power P depending on the MCS, the data rate R_{b}, the noise power spectral density (PSD) N_0, and the responsivity R of the photodiode. In Section IV, we will discuss two Wi-Fi LC specific problems. Finally, the noise sources and receiver sensitivities are discussed in Sections V (for RF) and VI.

II. Transmitter, Receiver and basic modeling

Fig.1 shows the block diagram of the Tx and Rx. We generally assume that up- and down-conversion to and from

979-8-3195-4420-9/26/$31.00 ©2026 IEEE

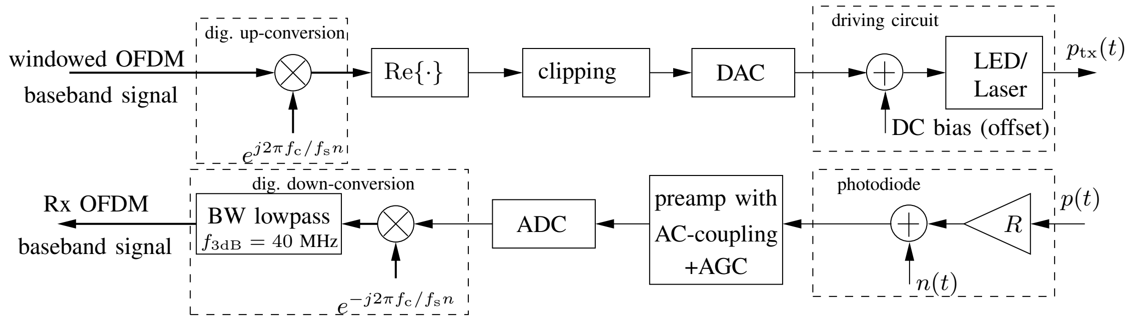

Fig. 1. Transmitter and receiver block diagram (BW: 5th order Butterworth IIR lowpass filter).

the subcarrier frequency f_c takes place in the digital domain. This ensures perfect I/Q balance and the absence of phase noise. For the analysis we assume that the DAC and the ADC operate at a sampling frequency of $f_s = 320$ MHz. Recent Wi-Fi7 chipsets support contiguous 320 MHz bands, so this assumption is realistic. The Nyquist frequency is therefore 160 MHz, which is why we only analyze Wi-Fi waveforms with 20, 40, or 80 MHz bandwidth. The clipping operation shown before the DAC limits the negative signal excursions of the real-valued passband waveform to keep the DC bias, that determines the average optical power, at a moderate level.

A photodiode converts the received optical signal $p(t)$ into a proportional current $Rp(t)$, where the responsivity R of silicon photodiodes is typically between 0.5 and 0.7 A/W in the defined wavelength range. The desired signal current is superimposed by an additive Gaussian distributed noise current $n(t)$. In the next section, we assume that $n(t)$ can be modeled as signal independent AWGN with a PSD N_0. This is the case when shot noise (see Section VI-A) dominates the noise.

For the simulative bit error rate (BER) analysis, we consider only the data fields of the packets. In doing so, we assume that the forward error correction (FEC) is based on LDPC codes, which is, for example, mandatory for the HE-PHY. The decoding is based on the belief propagation algorithm with 10 iterations, where the QAM demodulator delivers the approximate log-likelihood ratios of the data bits.

The Wi-Fi standards specify a packet error rate of 0.1 for determining the receiver sensitivity, with the packet length set at 4096 octets. This corresponds roughly to a BER of $P_b = 3 \cdot 10^{-6}$, which we use instead. We assume a LDPC codeword length of 1944, which applies to very long data packets. However, Table I also contains the required E_b/N_0-values for the smallest codeword length of 648 codebits, rendering it very easy to estimate the difference.

The MATLAB simulation results are based on perfect synchronization. For channel estimation, the long training fields (LTF) of the Wi-Fi packets are used [2], [3], but with deactivated noise[1]. The parameters E_b, i.e., the energy per bit, and N_0 are *always* electrical quantities, although they are measured in Ws (or W/Hz) in RF and A^2s (or A^2/Hz) for LC. However, in order to distinguish the power of the radiation that enters the receiver, we use P^{RF} and P (without additional labeling) for RF and LC, respectively.

[1]Any inadequacy in the channel estimation affects the whole packet.

III. IM/DD Modulation analysis

A. Known reference schemes

Uncoded on-off keying (OOK) based on rectangular pulses with a duration $T_b = 1/R_b$ equal to the bit interval is the by far simplest and most obvious transmission scheme for IM/DD. For equally likely bits, its BER is given as [4]

$$P_b = \frac{1}{2}\mathrm{erfc}\left(\frac{PR}{\sqrt{R_b N_0}}\right). \tag{1}$$

Note that (1) holds only for optimal detection. Assuming a BER $P_b = 3{\cdot}10^{-6}$, the minimum required optical power, which always depends on the parameters R_b, R, and N_0, is thus

$$P_{\min} = \mathrm{erfc}^{-1}(2P_b) \cdot \frac{\sqrt{R_b N_0}}{R} \approx 3.2 \cdot \frac{\sqrt{R_b N_0}}{R}.$$

The result already shows the very interesting relationship between P and R_b that holds for IM/DD, if the PSD of the noise current $n(t)$, see Fig. 1, is truly white. For a given MCS, increasing R_b by 2 results only in a $\sqrt{2}$ increase of $P_{\min}$ [5].

Another interesting scheme is, of course, 4-PPM, since it is — or rather was — the transmission standard for IrDA interfaces at 4 Mbps [6]. These "point-and-shoot" interfaces were actually quite widespread. 4-PPM can achieve a 3 dB power advantage over OOK [5]. The minimum required power for *optimal soft decision* detection is given as

$$P_{\min} = \frac{1}{2}\mathrm{erfc}^{-1}(P_b) \cdot \frac{\sqrt{R_b N_0}}{R} \approx 1.65 \cdot \frac{\sqrt{R_b N_0}}{R}, \tag{2}$$

where 1.65, i.e., 2.2 dB, corresponds to the target BER that we use for Wi-Fi.

B. Analysis for Wi-Fi LC

In addition to a standard signal-space analysis [4], [7], the BER of OOK under the IM/DD constraint can also determined by examining the electrical E_b/N_0-ratio at the photodiode output and relating E_b to P. In this context, the relationship between the BER and E_b/N_0 for uncoded OOK according to $P_b = 0.5\mathrm{erfc}\sqrt{E_b/(2N_0)}$ is then simply assumed to be basic textbook knowledge. For the OOK signal defined in Section III-A, as the signal component of the current is either

0 or $2PR$, its mean E_b-value is $T_\mathrm{b} \cdot (2PR)^2/2$, which leads to the same result as shown in (1).

For Wi-Fi LC, we will also assume that the required E_b/N_0-ratio of the currents is known for the respective MCSs in the AWGN case. Once the mathematical relation between E_b and P has been established, the required optical power can be estimated. This allows the plausibility of the MATLAB simulation results to be verified.

In the case of LC, however, it must also be taken into account that the energy efficiency depends additionally on the relative number of the OFDM pilot tones and the length of the guard interval relative to the FFT interval. This is done by the OFDM energy (efficiency) loss factor γ^2. The required E_b/N_0-ratios in AWGN are shown in Table I for the target BER. The numbers listed in the 3rd column are the dB values without considering γ^2 for a selection of QAM modulation orders M and code rates r_c. These results were obtained using MATLAB just by simulating the QAM signal vectors in AWGN. It should be noted that the results are all within a 3 dB range from the Shannon limits for equally likely QAM modulation symbols.

So, how is E_b related to P? We assume that the instantaneous optical power $p(t)$ consists of a DC part P (that results from a bias/offset in the LED driving current) and an AC part $p_\sim(t)$ ensuring $p(t) \geq 0$, i.e.,

$$p(t) = P + p_\sim(t) = P + \frac{s_\sim(t)}{R}, \text{ where } p_\sim(t) \geq -P. \quad (3)$$

Clearly, $p_\sim(t)$ results from the AC component in the LED (or laser) driving current and represents the *real-valued* OFDM passband signal to be transmitted. If the photodiode at the receiver input is AC coupled via a capacitor (e.g, to suppress the possibly very large DC current that has been caused by the received background light), the resulting OFDM signal current is just $s_\sim(t) = Rp_\sim(t)$. As the mean energy per bit

$$E_\mathrm{b} = \overline{s_\sim^2(t)} \cdot T_\mathrm{b} = \overline{s_\sim^2(t)}/R_\mathrm{b}$$

of the current $s_\sim(t)$ determines the BER, its second moment $\overline{s_\sim^2(t)}$ needs to be related to P to find — for given parameters R_b, R, and N_0 — the minimum required power P_min. On the one hand, E_b increases linearly with $\overline{s_\sim^2(t)}$; on the other hand, however, $s_\sim(t)/R$ must not and cannot have any negative excursions exceeding $-P$, as $p(t)$ is non-negative.

As OFDM is a parallel transmission scheme using a very large number of tones (subcarrier frequencies), an OFDM signal tends to be Gaussian distributed and large signal amplitudes will occur. However, if very large negative overshoots are clipped, which is possible if the effects due to the resulting nonlinear distortions on the BER are compensated by means of efficient FEC, then $s_\sim(t)$ may still contain enough electrical power/energy at a given optical power P.

A common approach [8] is to clip all negative signal excursions of the passband OFDM signal at the transmitter, see Fig. 1, that exceed a (non-integer) multiple k_clip of its standard deviation. If we assume — just for the analytical estimation of P_min — that the clipping will only have a little effect on the signal's standard deviation, we can express the maximum *negative* excursion of $s_\sim(t) = p_\sim(t)R$ as

$$-PR = -k_\mathrm{clip}\sigma_\sim$$

and $\sigma_\sim$ as the (almost exact) standard deviation of $s_\sim(t)$, i.e.,

$$\sigma_\sim = \sqrt{\overline{s_\sim^2(t)}} = \sqrt{E_\mathrm{b}R_\mathrm{b}}.$$

These two equations show the required relation between P and E_b. Therefore, as we already know the minimum required E_b/N_0-ratio of a Wi-Fi signal $s_\sim(t)$ that is *only* affected by AWGN, we can immediately provide the lower limit of the required *optical* power at the target BER, i.e.,

$$P_\mathrm{min} = \frac{k_\mathrm{clip}\sigma_\sim}{R} \geq k_\mathrm{clip}\sqrt{\left.\frac{E_\mathrm{b}}{N_0}\right|_\mathrm{req}} \cdot \frac{\sqrt{R_\mathrm{b}N_0}}{R}. \quad (4)$$

The equal sign in (4) holds, if k_clip is chosen to be large enough that clipping noise is negligible compared to the noise current $n(t)$. The comparison of (4) with the results in Section III-A shows that the term

$$k_\mathrm{clip}\sqrt{(E_\mathrm{b}/N_0)|_\mathrm{req}}$$

replaces $0.5 \cdot \mathrm{erfc}^{-1}(P_\mathrm{b}) = 1.65$ that holds for 4-PPM.

C. Simulation results

The dependency of the BER on the ratio $PR/\sqrt{N_0R_\mathrm{b}}$ is shown in Fig. 2 (a) for the HE PHY (i.e., Wi-Fi6) and various MCSs. For 20 MHz (40 MHz) HE waveforms with a normal 0.8 μs guard interval, the dB value of the OFDM energy loss factor γ^2 is given as

$$10\log_{10}\gamma^2 = 10\log_{10}\frac{242}{242-8} \cdot \frac{(4\cdot 3.2 + 0.8)\ \mu\mathrm{s}}{4 \cdot 3.2\ \mu\mathrm{s}} \approx 0.41\ \mathrm{dB},$$

as 8 (16) pilots tones are used in a 242 (484) tone recourse unit [3]. For a 80 MHz HE waveform with a 996 tone recourse unit, only 16 pilots tones are used. However, the dB change in γ^2 is negligible.

The results presented in Fig. 2 (a) include the clipping distortion and the effects of the up- and down-conversion to and from the center frequency f_c, which has been set to 26 MHz for the 20 MHz and to 56 MHz for the 80 MHz waveform, which is only shown for $M = 1024$. A 2nd order Butterworth highpass filter with a cut-on frequency of 2 MHz has also been considered.

The clipping factor k_clip has been set to 2.9 for all QAM orders ≤ 256. The reason will be explained in the next section. Only at $M = 1024$, $k_\mathrm{clip} = 3.4$ has been chosen[2]. Here — and only here — the clipping noise sets the minimum possible value of k_clip.

The results in Fig. 2 (a) show: if we switch, for example, from $M = 4$ and $r_\mathrm{c} = 1/2$ to $M = 64$ and $r_\mathrm{c} = 5/6$, then

[2]Notice that adaptive clipping is not possible, partly because, starting with Wi-Fi 6, a data frame can contain multiple resource units (RUs) with different modulation orders. And then a RU with $M = 1024$ would determine the bias for the whole frame. However, we consider $M = 1024$ to be less attractive, since R_b increases by only 10/8 compared to $M = 256$, while P_min increases by approximately $3.5 + 5\log_{10}1.25 = 4$ dB.

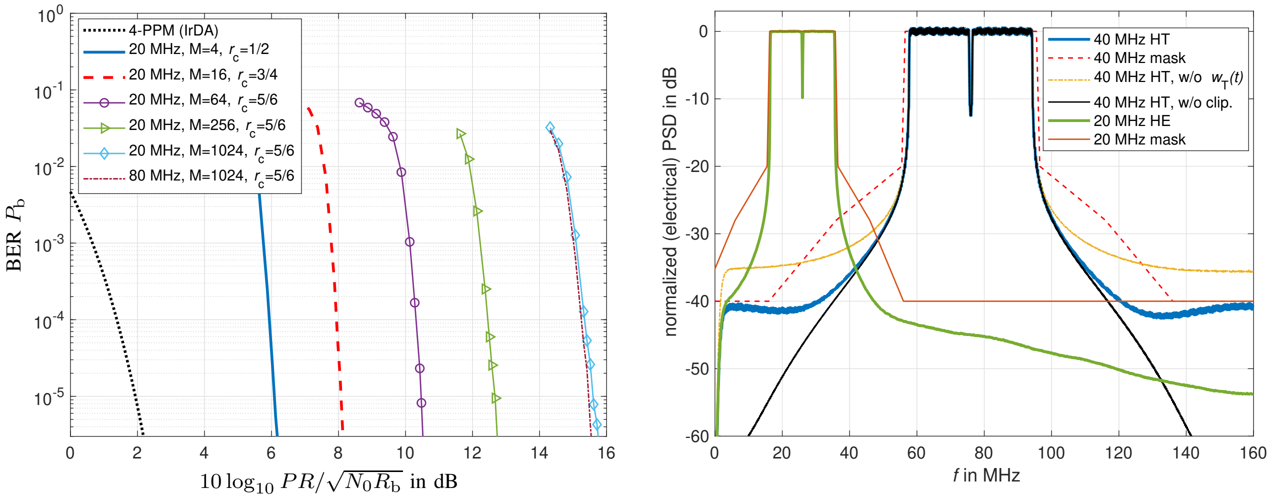

(a) (b)

Fig. 2. (a) Power efficiency for various MCSs and a HE waveform with $10\log_{10}\gamma^2 \approx 0.41$ dB. For QAM modulation orders $4 \leq M \leq 256$, $k_{\text{clip}} = 2.9$. For $M = 1024$, it is 3.4. The ratio on the x-axis is equivalent to the $E_{\text{b}}/N_0 = P^{\text{RF}}/(N_0 R_{\text{b}})$-ratio used in RF. (b) Electrical PSDs of a 40 MHz HT and a 20 MHz HE packet ($f_{\text{c}} = 76$ MHz and 26 MHz) for $k_{\text{clip}} = 2.9$. The effect of the windowing function $w_T(t)$ with and w/o clipping is also shown.

we need 4.4 dB more power at the Rx input, if we (would) keep R_{b} constant. If we now insert concrete values for N_0, R, and the data rate, which also depends on M, r_{c}, and the waveform bandwidth, we can estimate the receiver sensitivity.

How good is the analytical estimation according to (4)? An example with $M = 256$ proves that (4) allows for very accurate predictions. For $k_{\text{clip}} = 2.9$, that corresponds to 4.6 dB, and according to the third column of Table I, the estimation is $4.6 + (15.7 + 0.41)/2 = 12.7$ dB which is only a tiny bit less than the value shown in Fig. 2 (a) for the target BER.

Fig. 2 (a) also contains the BER plot of 4-PPM in AWGN. The surprisingly good performance shows that 4-PPM has been a very good choice for IrDA point-to-point links. Even if the modulation order in LC OFDM remains limited to 4, and even if a state-of-the-art LDPC code with $r_{\text{c}} = 1/2$ is employed, 4-PPM is nevertheless 4 dB more efficient in terms of the required optical power. The reason for OFDM's inferior performance is, of course, the required DC bias. Moreover, this consideration does not even take into account that the driver circuit in 4-PPM exhibits a significantly higher energy efficiency, because the driver transistor operates in switching mode — much like a Class-D amplifier. Consequently, when a current pulse is generated, (almost) no voltage drops across the transistor. For OFDM, however, the driver must operate in the linear region, and a large portion of the power supply energy is simply dissipated by the driver transistor as heat [9].

IV. Specific problems

A. Clipping threshold and spectral mask

What has been the reason to set k_{clip} to 2.9? The perhaps surprising answer is: as long as the QAM modulation order is not larger than 256, the decisive factor for choosing k_{clip} is not the impact of the clipping distortion on the BER[3] but rather on the signals (electrical) PSD. Clipping is a non-linear process and as such it leads to a spectral re-growth, so that the relevant spectral mask may no longer be adhered to. This is shown in Fig. 2 (b). Our analyses reveal that, from the perspective of the spectral masks that must be met, k_{clip} cannot be chosen to be less than approximately 2.9. In this case, two access points that operate at different center frequencies f_{c} will satisfy the Wi-Fi interference criteria.

It is important to note that, from the perspective of the spectral mask, a pulse-shaping function $w_{\text{T}}(t)$ must be applied to each OFDM symbol before mixing to smooth the transitions between the symbols. The function $w_{\text{T}}(t)$ is described in [3]. We found that a transition time of $T_{\text{TR}} = 100$ ns is sufficient.

B. Spectral Leakage

Our simulations have clearly shown that the down-conversion at the Rx *essentially* requires a digital lowpass filter. This filter attenuates the spectral components that have been cyclically shifted from $-f_{\text{c}}$ to $-2f_{\text{c}}$ due to the time domain multiplication of the sampled input signal with $\exp(-j2\pi f_{\text{c}}/f_{\text{s}}n)$, where n is the time index. Since the standard conform center frequencies (and thus also $-2f_{\text{c}}$) are relatively small compared to the signal bandwidths, yet are not integer multiples of the subcarrier spacing, which is either 312.5 kHz or 312.5/4 kHz, leakage occurs if the filter is omitted. It is important to remember that the FFT performs a rectangular windowing as a part of the correlation. In other words, the tones around $-2f_{\text{c}}$ are not orthogonal to the desired tones around DC, as the FFT-window does not include an integer number of cycles for these interfering tones. Especially

[3] According to our MATLAB simulations, if the mask would be ignored for $M = 256$, a further reduction of k_{clip} could provide a modest optical gain of 0.25 dB. So at $M = 256$ and $k_{\text{clip}} = 2.9$, the clipping noise is relatively close at the BER limit.

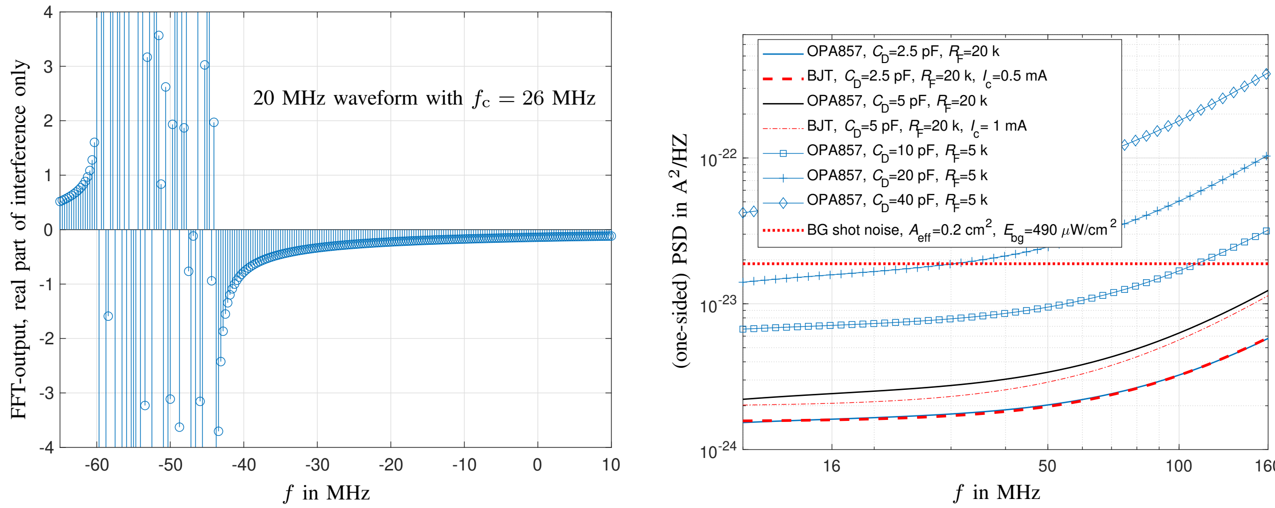

(a) (b)

Fig. 3. (a) Digital down-conversion requires lowpass filtering to suppress the spectral components around $-2f_c$ before the FFT (and thus a rectangular windowing) is applied. Otherwise, since $-2f_c$ is not an integer multiple of the subcarrier spacing, the desired FFT output around DC will suffer from interference caused by leakage. The plot shows the interference part of the FFT output for $M = 256$, if no lowpass filter is used. (b) PSD of the input referred preamp noise current for different photodiode capacitances of a state-of-the-art ultra low noise transimpedance amplifier (TI OPA857) based on BICMOS.

at $M = 256$ or $M = 1024$, the leakage leads to very strong interference, if the filter is not used, see Fig. 3 (a). And this interference would also skew the channel estimation which is based on the LTF in the preamble.

The effects have been mentioned before [10], [11], although somewhat misleadingly described as aliasing. However, the problem wouldn't arise at all if the subcarrier frequencies of the real-valued passband signal were integer multiples of the subcarrier spacing (as in discrete-multitone transmission) — even if subcarriers near DC were utilized.

In the proposed system approach shown in Fig. 1, we suggest a 5th order Butterworth lowpass filter with a fixed 3 dB cutoff frequency of 40 MHz. If it is assumed that a $B = 20$ MHz waveform is used, the standard conform center frequencies $f_c \in \{26, 46, 66, 86, 106, 126\}$ MHz allow operation within the 160 MHz Nyquist frequency limit. For $f_c = 26$ MHz, the worst case (with respect to the interference rejection) appears, as $-2f_c + B/2$ is only -42 MHz, i.e., very close to the filter edge. This is the reason why the performance of the 20 MHz waveform has been additionally compared to the 80 MHz waveform with $f_c = 56$ MHz in Fig. 2. Here, $-2f_c + B/2$ is equal to -76 MHz, which is clearly within the stop band of the filter. Fortunately, even for the worst case with $f_c = 26$ MHz and $M = 1024$, the penalty is very small.

However, if another access point uses a directly adjacent channel, does spectral leakage occur in that case as well, and is it not *much* stronger? (That would also happen in an RF OFDM system.) The answer is no, due to the Wi-Fi channel grid, the *difference* between two center frequencies is always an integer multiple of the subcarrier spacing.

V. Noise in RF

In order to estimate the Rx sensitivities for the various MCSs, N_0 must be known.

First, it is helpful to consider noise in RF. The thermal noise picked up by the antenna can be assumed to be independent of the antenna gain, as the thermal radiation of the environment is basically isotropic [12]. If an amplifier with a noise figure $F_{\mathrm{dB}} = 10\log_{10} F$ is assumed, N_0 is given as

$$N_0 = k_{\mathrm{B}}T + k_{\mathrm{B}}T_{\mathrm{ref}}(F-1), \qquad \text{in W/Hz}, \tag{5}$$

where k_{B} is Boltzmann's constant. At a temperature T that is equal to the reference "earth" temperature $T_{\mathrm{ref}} = 290$ K, $k_{\mathrm{B}}T$ corresponds to -114 dBm/MHz. As $(E_b/N_0)|_{\mathrm{req}}$ is known from Table I, the theoretical RF Rx sensitivity is

$$P^{\mathrm{RF}}_{\mathrm{min,dBm}} \approx -114 + \left.\frac{E_b}{N_0}\right|_{\mathrm{req,dB}} + F_{\mathrm{dB}} + 10\log_{10}\big(R_b(\mathrm{Mbps})\big)\ \mathrm{dBm}.$$

Table I shows the results for a 20 MHz HE waveform with a 0.8 μs guard interval and a reasonable noise figure of 6 dB. It is interesting to note that for all MCSs, there is always a margin of approximately 13 dB compared to the standardized required values[4].

The required irradiance shown in the rightmost column of Table I is not given in the standard [3]. We calculated it based on the *specified* Rx sensitivity values, an antenna gain of 3 dB, and a carrier frequency of 6 GHz. This leads to an effective detector (antenna) area of approximately $4\ \mathrm{cm}^2$.

VI. Noise in LC

A. Ambient light induced shot noise

In fact, the PSD $k_{\mathrm{B}}T$ of the thermal noise in (5) is only an approximation for

$$hf/\left(e^{\frac{hf}{k_{\mathrm{B}}T}} - 1\right), \tag{6}$$

[4]At least for lower modulation orders, this seems to be large. However, Wi-Fi4 systems with HT waveforms may use convolutional codes for FEC, which exhibit a penalty of up to 3 dB compared to LDPC codes [2]. As the loss γ^2 is also larger [2], the margin then decreases to about 9 dB.

			20 MHz PPDU (HE-format, 242 tone RU, 0.8 μs GI, $f_c = 6$ GHz)			
modulation order M	FEC code rate r_c	required $\frac{E_b}{N_0}/\gamma^2$ (dB)	data rate R_b (Mbps)	theor. sens. $P^{RF}_{min,dBm}$ (dBm)	specified sens. $P^{RF}_{min,dBm}$ (dBm)	result. requir. irradiance E^{RF}_{min} (μW/cm^2)
2	1/2	2.7 (3.05)	8.6	-95.5	-82	$1.6 \cdot 10^{-6}$
4	1/2	2.7 (3.05)	17.2	-92.5	-79	$3.2 \cdot 10^{-6}$
4	3/4	3.4 (4.2)	25.8	-90.1	-77	$5 \cdot 10^{-6}$
16	1/2	5.2 (5.7)	34.4	-87	-74	$10 \cdot 10^{-6}$
16	3/4	6.7 (7.4)	51.6	-83.7	-70	$25 \cdot 10^{-6}$
64	3/4	10.3 (11.2)	77.4	-78.4	-65	$8 \cdot 10^{-5}$
64	5/6	11.4 (12.2)	86	-76.8	-64	$1 \cdot 10^{-4}$
256	5/6	15.7 (16.5)	114.7	-71.3	-57	$5 \cdot 10^{-4}$
1024	5/6	20.2 (21.2)	143.4	-65.8	-52	$1.6 \cdot 10^{-3}$

TABLE I

RECEIVER SENSITIVITIES IN RF FOR VARIOUS MCS, A 20 MHZ HE WAVEFORM AND 1 SPATIAL STREAM. THE VALUES IN THE PARENTHESES IN THE THIRD COLUMN ASSUME A 648 BIT LDPC CODEWORD LENGTH (INSTEAD OF 1944 BITS). DOUBLING THE BW LEADS TO A 3 dB PENALTY.

		HE-format, 0.8 μs guard interval, $E_{bg} = 490$ μW/cm^2, $R = 0.6$ A/W, $A_{eff} = 0.2$ cm^2						
			242 tone RU			996 tone RU		
modul. order M	code rate r_c	required $\frac{PR}{\sqrt{N_0 R_b}}$ (dB)	data rate R_b (Mbps)	theor. sens. $P_{min,dBm}$ (dBm)	on-axis E_{min} (μW/cm^2)	data rate R_b (Mbps)	theor. sens. $P_{min,dBm}$ (dBm)	on-axis E_{min} (μW/cm^2)
2	1/2	6.2	8.6	-40.5	0.44	36	-37.4	0.90
4	1/2	6.2	17.2	-39	0.63	72.1	-35.9	1.28
4	3/4	6.5	25.8	-37.8	0.82	108	-34.7	1.7
16	1/2	7.5	34.4	-36.2	1.2	**144.1**	-33.1	**2.5**
16	3/4	8.2	51.6	-34.6	1.7	216.2	-31.5	3.5
64	3/4	10	77.4	-32	3.2	324.3	-28.9	6.5
64	5/6	10.6	86	-31.1	3.9	360.2	-27.9	8.1
256	5/6	12.8	114.7	-28.3	7.4	480.4	-25.2	15.1
1024	5/6	15.8	**143.4**	-24.8	**16.5**	600.5	-21.9	32.2

TABLE II

RX SENSITIVITIES IN LC FOR VARIOUS MCSS. ONLY SHOT NOISE CAUSED BY AMBIENT LIGHT IS CONSIDERED FOR A SMALL PHOTODIODE THAT FITS INTO A MOBILE PHONE. THE NUMBERS HIGHLIGHTED IN BOLD SHOW THAT, FOR $M > 4$, INCREASING B IS MORE EFFICIENT THAN INCREASING M.

where h is Planck's constant. Equation (5) is the "Nyquist approximation" [12] that holds for $hf \ll k_B T$. For optical frequencies, the thermal noise of the radiation is negligible. As can be seen from (5), the noise figure always refers to the thermal noise $k_B T$ of the radiation at $T = T_{ref}$. This shows that the concept of a noise figure does not apply to LC.

In contrast, the quantum nature of the light leads to a randomness in the photon stream, which is transformed into a fluctuating current $n(t)$. Assuming that ambient light with a constant optical power $P_{bg} \gg P$ is received, the corresponding DC-current $P_{bg}R$ is superimposed by AWGN $n(t)$ with a PSD

$$N_0 = 2qRP_{bg} \qquad \text{in A}^2/\text{Hz}, \tag{7}$$

where q is the electron charge. Although (7) looks simple, the difficulties compared to RF become apparent as P_{bg} depends on many factors. There is no "reference noise" with a concrete value of the PSD. Rather, P_{bg} and thus N_0 depend on many factors. The strongest source of shot noise is sun light. Therefore, P_{bg} varies over day time, season, and the receiver position and orientation in the room, for example, and it is difficult to give typical values. Sure, P_{bg} also depends on design parameters like the responsivity R of the photodiode (which can only partially controlled) and the effective area A_{eff}, field of view (FOV), and spectral width of the optical frontend.

The LC standard defines that each receiver must be sensitive to the entire 800-1000 nm wavelength range [1]. Although it also highlights the possibility to use 2 Rx chains, where one covers the range from 800 to 900 nm and the other from 900 to 1000 nm, we assume that the Rx cannot separate the spectral bands. The 2 chains approach does not only require two physical receivers in parallel, and thus more space, it also demands for optical interference filters. Such filters are very difficult to fabricate, as the center wavelength of planar filters varies over the angle of incidence of the radiation [13]. The potential optical gain of a 100 nm interference filter compared to an absorption filter (like Schott RG780) would be also low.

B. Sensitivity of a very small 20 mm^2-receiver in shot noise

So, unlike in RF, there is not "just one" N_0; rather, assumptions must be made about the detector area and the shape of the reception characteristic. As an example, we assume that the detector is to be mounted on the top of a mobile phone's casing and that the detector area is 20 mm^2. In some cases, two smaller photodiodes may be placed side by side but connected to a single preamplifier. The half intensity point should be located at a direction angle of approximately 25°. This angle lies precisely within the range of the IrDA interface specification [6]. The IrDA standard defines, that a receiver must function properly at a background light irradiance of

$E_{\mathrm{bg}} = 490\ \mu\mathrm{W/cm}^2$ in the sensitive wavelength range [6]. To obtain the sensitivities in Table II, this value has been used along with $R = 0.6$ A/W. Even with this very small area, which yields a value of $N_0 = RE_{\mathrm{bg}}A_{\mathrm{eff}} \approx 2 \cdot 10^{-23}\ \mathrm{A}^2/\mathrm{Hz}$, the sensitivities of the MCSs are orders of magnitude worse than those of RF. But what happens if no ambient light is present? In this case, we need to consider the noise generated by the preamplifier itself.

C. *Preamplifier noise*

Instead of the noise figure, we consider the input referred noise of a transimpedance amplifier with the feedback resistor R_{F}. For a bipolar-junction transistors (BJT), the one-sided PSD of the input-referred noise is (approximately) given by

$$S(f) = 2qI_{\mathrm{b}} + 4k_{\mathrm{B}}T\left(\frac{1}{R_{\mathrm{F}}} + R_{\mathrm{bb}}(2\pi C_{\mathrm{D}}f)^2\right) + \frac{2qI_{\mathrm{c}}(2\pi C_{\mathrm{t}}f)^2}{g_{\mathrm{m}}^2},$$

where C_{t} is the sum of the photodiode capacitance C_{D} and the capacitances C_{EB} and C_{CB} of the BJT [14]. Although the collector current I_{c} and the base spreading resistor R_{bb} are sources of white noise at their given positions, referred to the input these noise currents exhibit a f^2-dependency, where the contribution due to I_{c} can be controlled via the transconductance $g_{\mathrm{m}} \approx I_{\mathrm{c}}/28\ \mathrm{mV}$. (The term I_{b} is the base current.)

Fig. 3 shows a PSPICE simulation of this PSD for a state-of-the-art transimpedance amplifier (TI OPA857) based on BICMOS depending on C_{D} and R_{F}. For comparison, the PSD of the shot noise with $N_0 = 2 \cdot 10^{-23}\ \mathrm{A}^2/\mathrm{Hz}$ is also shown, just like the PSD according to the analytical expression above (only for $C_{\mathrm{D}} = 2.5$ and 5 pF; data from the SiGe transistor BFP740 has been used). It is apparent that for $C_{\mathrm{D}} < 10$ pF a slightly better noise performance as supposed for Table II can be obtained, although it is unclear weather current Wi-Fi chips estimate the frequency dependency of the noise (that would be required for optimal LDPC decoding performance) or not.

It can be proven that the thickness of the i-layer in PIN photodiodes, which are designed to have a flat amplitude response up to approximately 150–200 MHz at a reverse voltage of 30 V, is limited to about 100 μm[5]. This yields a capacitance of approximately 1 pF/mm^2. So if the diode (which has been assumed for the previous example) exhibits a focusing lens, its capacitance actually remains below 10 pF.

D. *A simple Wi-Fi Direct Link*

It is obvious that — given the constraint of ambient light induced shot noise — a factor 2 increase of A_{eff} leads to a 1.5 dB drop in $P_{\mathrm{min,dB}}$. It is therefore more appropriate to consider the required (on-axis) irradiance [6], [16]

$$E_{\mathrm{min}} = P_{\mathrm{min}}/A_{\mathrm{eff}}$$

at the input of the optical interface instead of P_{min} alone. The corresponding values for the shot noise PSD level of $2 \cdot 10^{-23}\ \mathrm{A}^2/\mathrm{Hz}$ are also included in Table II for LC, where no margins have been considered. For a link budget, however, a margin is required that accounts for implementation imperfections[6]. A value of 4 dB (optical) will be used.

We consider a 80 MHz HE packet with $M = 64$, $r_{\mathrm{c}} = 5/6$, and $R_{\mathrm{b}} = 360.2$ Mbps. The required irradiance at the Rx input is thus $8.1 \cdot 10^{0.4} \approx 20\ \mu$W/cm^2. Under the assumption of a "Wi-Fi Direct" point-to-point link between two mobile devices over a distance of 100 cm, the required Tx radiant intensity I_{tx} is $I_{\mathrm{tx}} = 20 \cdot 100^2\ \mu\mathrm{W/srad} = 200\ \mathrm{mW/srad}$. For a port with a half intensity angle of $\phi_{\mathrm{H}} = 25°$ (half angle of the cone) and a generalized Lambertian characteristic [17], this corresponds to an *optical* Tx power

$$P_{\mathrm{tx}} = I_{\mathrm{tx}} \cdot 2\pi/(n+1),\ \text{with}\ n = -\log(2)/\log(\cos(\phi_{\mathrm{H}})),$$

of 160 mW. Of course, this value requires both devices to be perfectly aligned. On the other hand, the ambient light may also be dimmer than expected.

E. *Communicating with an access point*

We continue with the example and assume that a connection is to be established between a mobile phone/station (MS) and an access point (AP) located 4 m away. The AP must then generate a radiant intensity $I_{\mathrm{tx,AP}}$ of at least $16 \cdot 200\ \mathrm{mW/srad} = 3\,200\ \mathrm{mW/srad}$. In order to ensure coverage with a large FOV, such values require multiple narrow cone transmitters — each, for example, with $\phi_{\mathrm{H}} = 25°$ — that are oriented in different directions. Depending on the maximum power dissipation, it may even be necessary to employ multiple parallel transmitters for each direction.

The Rx is even more complicated. We also assume here that several narrow cone ports — each with $\phi_{\mathrm{H}} = 25°$ — are oriented differently to ensure the same shapes of the emission and reception characteristics. (An imaging receiver [5] with a large-area lens system could be used as an alternative.) However, in order to guarantee system parity [16], i.e., $E_{\mathrm{min,MS}} \cdot I_{\mathrm{tx,MS}} = E_{\mathrm{min,AP}} \cdot I_{\mathrm{tx,AP}}$, we certainly cannot assume that the detector areas are increased by a factor 16^2 each to reduce $E_{\mathrm{min,AP}}$ by 16. Therefore, it will very likely be necessary to lower the modulation order in the uplink as well — to, for example, $M = 4$. For $M = 4$, $r_{\mathrm{c}} = 3/4$ and a 80 MHz bandwidth, R_{b} is still 108 Mbps. As a result, $E_{\mathrm{min,AP}}$ would have already decreased by a factor of $8.1/1.7 = 4.76$, cf. Table II, so that the necessary increase in detector area would amount to only $(16/4.76)^2 \approx 11.3$. The required detector area for each of differently oriented ports at the AP would then be approximately 2.3 cm^2. To manage the f^2-noise component of the preamplifier at a very high photodiode capacitance , cf. Fig. 3 (b), it will still be necessary to employ multiple parallel diodes for each direction, each operating with its own dedicated preamplifier.

[5]At the corresponding electric field, the speed of the electrons is then approximately 33 μm/ns. However, the holes, that are generated deeper within the layer as the wavelength increases, are slower, see also Chapter 17 in [15].

[6]Furthermore, if a laser is going to be used, the laser threshold must also be considered, as it increases the DC bias P.

VII. Conclusions

The change from carrier frequencies in the 5 or 6 GHz range to optical frequencies is more challenging than it appears at a first glance. In fact, light communication is based on intensity modulation and direct detection, and the physics — which describe, for example, radiation detection — are entirely different. It is not simply a matter of replacing radio antennas with optical "antennas" (a term used in Amendment 802.11bb); rather, a photodiode generates a current that is proportional to the optical power. The theory of noise in optical direct detection (without any optical preamplifier) is entirely different from that in RF. Even if one circumvents certain difficulties — such as the interference caused by the leakage effect — the challenge of a poor receiver sensitivity remains, particularly if one interprets the term more generally as "required power per unit area". Optical radiation can be focused easily to compensate the sensitivity problem by reducing the path loss, which is ideal for short-range point-to-point links like Wi-Fi Direct. However, for an access point to achieve coverage over distances $\gg 1$ m using angle diversity (with multiple, differently oriented optical ports), the transceivers become highly complex, in comparison quite bulky, difficult to install, power-hungry, and expensive. Such access points are primarily of interest for difficult industrial applications, where RF does not work, and where the mobile stations, e.g., in the form of robots, have much fewer restrictions in terms of size, power consumption, and costs, than for consumer applications.

References

[1] IEEE Standards Association, *Part 11: Wireless LAN Medium Access Control (MAC) and Physical Layer (PHY) Specifications, Amendment 6: Light Communications*, 2023, IEEE Std 802.11bb$^{\mathrm{TM}}$-2023.

[2] E. Perahia and R. Stacey, *Next generation wireless LANs : 802.11n and 802.11ac*, Cambridge Univ. Press, 2nd edition, 2013.

[3] IEEE Standards Association, *Part 11: Wireless LAN Medium Access Control (MAC) and Physical Layer (PHY) Specifications, Amendment 1: Enhancements for High-Efficiency WLAN*, 2021, IEEE Std 802.11ax$^{\mathrm{TM}}$-2021.

[4] M. Wolf and M. Haardt, "Comparison of OFDM and Frequency Domain Equalization for Dispersive Optical Channels with Direct Detection," in *Proc. 14th Int. Conf. on Transparent Optical Networks*, Coventry, UK, July 2012.

[5] J. M. Kahn and J. R. Barry, "Wireless Infrared Communications," *Proceedings of the IEEE*, pp. 265–298, Feb. 1997.

[6] Infrared Data Association (IrDA), *Serial Infrared Physical Layer Specification*, 2001, Version 1.4.

[7] J. R. Barry, E. A. Lee, and D. G. Messerschmitt, *Digital Communication*, Springer Science+Business Media, third edition, 2004.

[8] J. Armstrong and B. J. C. Schmidt, "Comparison of Asymmetrically Clipped Optical OFDM and DC-Biased Optical OFDM in AWGN," *IEEE Communications Letters*, vol. 12, no. 5, pp. 343–345, May 2008.

[9] J. R. García-Meré, J. Rodríguez, D. G. Lamar, and J. Sebastián, "On the Use of Class D Switching-Mode Power Amplifiers in Visible Light Communication Transmitters," *Sensors*, vol. 22, no. 13, pp. 1–19, June 2022.

[10] A. A. Purwita and H. Haas, "Studies of Flatness of LiFi Channel for IEEE 802.11bb," in *2020 IEEE Wireless Communications and Networking Conference (WCNC)*, 2020, pp. 1–6.

[11] E. Khorov and I. Levitsky, "Current Status and Challenges of Li-Fi: IEEE 802.11bb," *IEEE Communications Standards Magazine*, vol. 6, no. 2, pp. 35–41, 2022.

[12] J. J. Condon and S. M. Ransom, *Essential Radio Astronomy*, Princeton University Press, 2016.

[13] J. R. Barry and J. M. Kahn, "Link design for nondirected wireless infrared communications," *Applied Optics*, vol. 34, no. 19, pp. 3764–3776, July 1995.

[14] E. Säckinger, *Broadband Circuits for Optical Fiber Communication*, Wiley, 1 edition, 2005.

[15] B. E. A. Saleh and M. C. Teich, *Fundamentals of Photonics*, John Wiley & Sons, Inc., 1991.

[16] F. R. Gfeller and W. Hirt, "A Robust Wireless Infrared System with Channel Reciprocy," *IEEE Communications Magazine*, pp. 100–106, Dec. 1998.

[17] F. R. Gfeller and U. Bapst, "Wireless In-House Data Communication via Diffuse Infrared Radiation," in *Proc. of the IEEE*, 1979, vol. 67, No. 11, pp. 1474–1486.